

Article

Direct Driven Hydraulic System for Skidders

Juraj Benić , Juraj Karlušić *, Željko Šitum, Mihael Cipek  and Danijel Pavković 

Faculty of Mechanical Engineering and Naval Architecture, University of Zagreb, Ivana Lučića 5, 10000 Zagreb, Croatia; juraj.benic@fsb.hr (J.B.); jzeljko.situm@fsb.hr (Ž.Š.); mihael.cipek@fsb.hr (M.C.); danijel.pavkovic@fsb.hr (D.P.)

* Correspondence: juraj.karlusic@fsb.hr

Abstract: This paper investigates potential uses of a novel direct driven electro-hydraulic systems for articulated forestry tractors (skidders), due to these systems having notably higher energy efficiencies compared to classical electro-hydraulic systems that are currently being used in skidders for steering, lifting the front and the rear plate, as well as for operating the double-drum winch. A detailed analysis of the skidder rear plate mechanism is carried out, and static force profiles of hydraulic cylinders are obtained for the rear plate based on mechanism dynamics and measurement data from the literature. Thus, obtained results have been used to emulate the real-life force profiles in laboratory experiments featuring both the classical and the proposed direct driven hydraulic systems for the purpose of comparative analysis of their energy and fuel efficiency. These results are subsequently used to estimate the skidder fuel consumption and possible fuel savings over the entire vehicle life span for the realistic vehicle utilisation scenario. The main result is that fuel consumption can be reduced up to five times in the case of direct driven hydraulic system, thus effectively resulting in return of investment period of about four years in the case of skidder being retrofitted with direct driven hydraulic system.



Citation: Benić, J.; Karlušić, J.; Šitum, Ž.; Cipek, M.; Pavković, D. Direct Driven Hydraulic System for Skidders. *Energies* **2022**, *15*, 2321.

<https://doi.org/10.3390/en15072321>

Academic Editors: Antonio Viguera-Rodríguez and Helena M. Ramos

Received: 25 February 2022

Accepted: 21 March 2022

Published: 23 March 2022

Publisher's Note: MDPI stays neutral with regard to jurisdictional claims in published maps and institutional affiliations.



Copyright: © 2022 by the authors. Licensee MDPI, Basel, Switzerland. This article is an open access article distributed under the terms and conditions of the Creative Commons Attribution (CC BY) license (<https://creativecommons.org/licenses/by/4.0/>).

Keywords: direct driven hydraulics; forestry tractor; skidder; efficiency; fuel savings

1. Introduction

Nowadays, there is an increasing demand for reducing the cost of running forestry machinery. In addition, the regulatory pressure is increased to reduce exhaust emissions so as to improve the ecological indices as well as to reduce acoustic noise [1] in order to comply with increasingly more stringent industry ergonomic guidelines [2]. Therefore, manufacturers of forestry equipment are increasingly interested in making their heavy machinery more efficient, which can be seen with the emergence of particular hybrid and electric powertrain-based forestry vehicles, mostly harvesters [3], as well as in the latest study on skidder hybridization [4,5]. However, most of the utility attachments and auxiliary systems (winches, buckets, etc.) for tractors, skidders and similar working machinery are being driven by hydraulics. For example, an articulated forestry tractor known as a skidder uses hydraulic steering, hydraulic lifting for front pushing plate or rear protection plate, and it also uses a hydraulic double-drum winch [6]. Those systems are driven by classical hydraulics that are controlled by means of proportional valves, whose utilisation results in notable disadvantages of these systems, primarily in terms of additional heat generation (heat losses), low overall efficiency and significant pressure losses.

Thus, it is of great importance to investigate the possibilities for efficiency improvement of hydraulic systems. This can either be done by means of hydraulic system optimisation or by means of modification of hydraulic system by replacing the low-efficiency components with more efficient ones. In that sense, the former approach may require detailed simulation analysis of the system's behaviour in the design stage, such as by using finite element method analysis (see, e.g., [7]), which may yield significant savings in terms of production costs for the same performance of hydraulic components [8]. On the other

hand, in the implementation phase, different metaheuristic optimization models can be used to provide an optimal solution to hydraulic system operation [9]. The comparative weaknesses and advantages of such optimisation tools have been assessed in [10].

Hardware-based efficiency improvement measures have recently included integration of direct driven hydraulic (DDH) systems, which have a more compact structure compared to conventional hydraulic systems, along with higher reliability and efficiency [11]. Integration of DDH systems in non-road mobile machinery (NRMM) has been receiving increasing attention recently, mainly with respect to potentials for reducing the energy consumption. Simulations and experiments of DDH systems implemented within some of the utility attachments, such as hydraulic crane [12], show promising results, especially in those cases where regeneration of kinetic and potential energy is possible. Prototype testing on an existing mining loader has shown that the overall efficiency of the direct driven hydraulic system can be much higher (up to 50%), with minimum steady-state control error achieved when paired with the fuzzy proportional-integral (fuzzy PID) controller [13]. Fuzzy logic in combination with sliding model control has also been proposed in [14] to account for inherent nonlinearities of hydraulic actuator dynamic model. Metaheuristic approaches have also been successfully employed for the hydraulic actuator control optimization tasks, such as the firefly metaheuristic algorithm [15], and genetic algorithm presented in [16]. Reference [17] proposed a hybrid optimisation algorithm for a hydraulic cylinder pressure self-tuning PID controller, wherein adaptation has been based on particle swarm optimisation (PSO) combined with genetic algorithm (GA). Although DDH introduces more complexity in terms of additional machinery and overall mass, the results of an investigation into these potential drawbacks for the case of an excavator arm and a boom have shown that better performance can be obtained with a DDH system compared to the case when classical hydraulic systems has been used [18]. The positive aspects of decentralization, which are made possible by the use of the DDH where hydraulic pumps are disconnected from the engine have been shown in [19]. For instance, the use of the DDH can facilitate efficiency increase from 8% up to almost 57% in the case of a small crane being driven by one hydraulic cylinder [20]. The effect of sub-zero temperatures on oil and energy efficiency of a DDH system is investigated in [21]. It has been shown that for temperatures below zero, high-performance oil has almost 10% higher efficiency than the conventional multi-grade oil. Different control methods for a DDH system are compared in [22] where PID controller achieved the highest energy efficiency while the sliding mode controller obtained faster dynamics with a slightly lower energy efficiency. The preliminary results presented in [23] showed that the DDH system could also greatly increase the overall efficiency of the skidder powertrain.

Having this in mind, this paper investigates possible uses of the direct driven hydraulic system on a skidder in order to increase the skidder operating efficiency. In particular, the DDH system would be used instead of classical hydraulics for the lowering and lifting of the skidder rear plate. In order to verify this hypothesis, forces acting upon hydraulic cylinders are obtained by analysing the rear plate mechanism. The topology of similar mechanical systems and their kinematics and dynamics [24,25] are used as a basis for the analysis conducted in this work. Both the classical and the direct driven electro-hydraulic systems are experimentally verified for the purpose of a comparative analysis of their efficiency. Experiments are carried out under laboratory conditions for different hydraulic cylinder loading scenarios, including the unloaded cylinder case and several cases of different cylinder payloads. The obtained results are used to gain insights about the possible advantages of the directly driven electro-hydraulic system in terms of energy efficiency compared to the utilization of classical proportional hydraulics. The presented results have indicated that an at least three-fold improvement in energy and fuel efficiency of the skidder powertrain can be achieved by using direct driven hydraulic systems for driving the rear plate mechanism compared to the case of classical hydraulics.

2. Analysis of the Static Cylinder Force of Skidder Rear Plate

This section outlines the hydraulic drive of the articulated forestry tractor (skidder) rear plate mechanical system and derives the overall mechanical system model by using the methodology of virtual work. Based on these results, static profiles of hydraulic cylinder forces are derived for different rear plate loads.

2.1. Outline of the Skidder Rear Plate Mechanical System

Skidders are essentially tractors repurposed for pulling cut trees in a process called skidding. They are protected with plates and equipped with a winch and an inevitable all-wheel drive. The skidder studied in this paper, EcoTrac 120V, was made by the Croatian company Hittner located in the town of Bjelovar [26]. It is a seven-ton skidder, equipped with a double drum winch. The above mentioned process of skidding is shown in Figure 1, in which EcoTrac 120V is pulling two logs at the same time. After being connected with winch cable, logs are pulled to the rear protective plate and are ready for transportation.



Figure 1. Skidder EcoTrac 120V in operation [27].

The skidder rear plate consists of five parts, which are illustrated in Figure 2. The skidder chassis (1) represents a ground part of the rear plate mechanism. Two double-acting asymmetrical hydraulic cylinders (2) are used as actuators for lowering and lifting the rear plate. The upper arm (3) is used as an interconnecting element between the hydraulic cylinder, the chassis and the rear plate (4). The lower arm (5) connects the rear plate with the chassis.

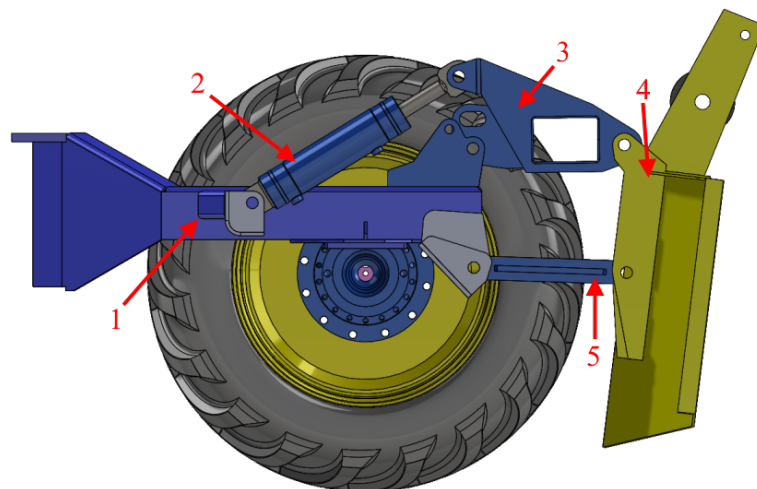


Figure 2. Skidder rear plate, courtesy of Hittner d.o.o.

The linkage mechanism of the skidder rear plate is shown in Figure 3. The hydraulic cylinder force (F_{cyl}) is the input force of the system, while F_h and F_v are horizontal and vertical components of the rope force. Dimension L refers to a cylinder length which includes piston length and housing length. The angles of the individual linkages are represented by φ_i where index i is the link number. The dimension of individual links are defined as l_i where index i is the link number as shown in Figure 3. Angles α_i , β_i and γ_i are angles of two triangle links. The relation between the cylinder and the rope forces will be derived by using the virtual work analysis.

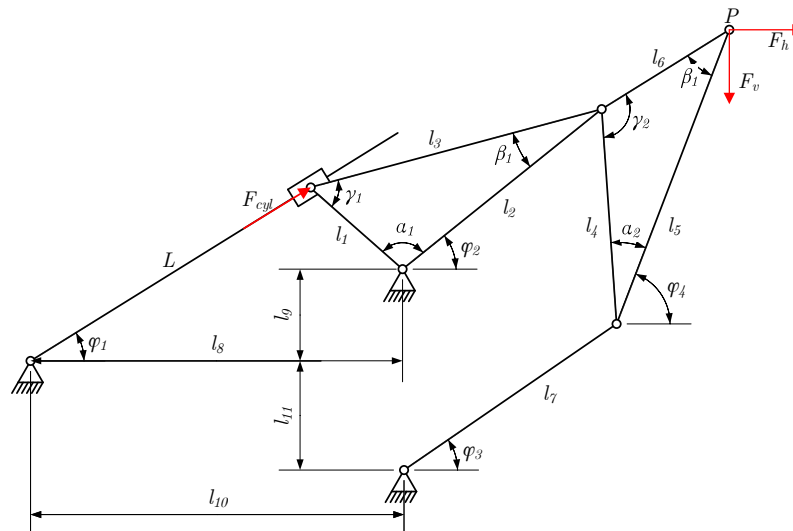


Figure 3. Linkage mechanism of the skidder rear plate.

2.2. Position Analysis

The analysis of the position of the proposed linkage mechanism is performed by means of vector loops as shown in Figure 4. Three vector loops are defined. From the first loop angle φ_2 is calculated, while angle φ_4 is obtained from the second loop. The coordinates of point P are calculated from the last loop.

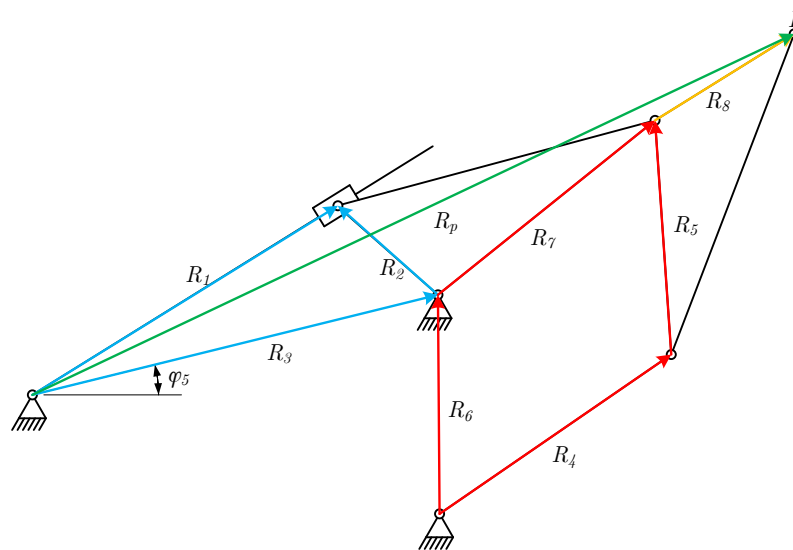


Figure 4. Position vector loops of the linkage mechanism for the skidder rear plate.

The first vector loop is given as:

$$R_1 - R_2 - R_3 = 0. \tag{1}$$

Using complex number notation for each position vector the above equation becomes:

$$Le^{j\varphi_1} - l_1e^{j\beta} - l_{R_3}e^{j\varphi_3} = 0, \quad (2)$$

where angle β is given as:

$$\beta = \alpha_1 + \varphi_2. \quad (3)$$

Two scalar equations are obtained from (2) by applying the Euler identity and are given as:

$$\begin{aligned} L \cos(\varphi_1) - l_1 \cos(\beta) - l_8 &= 0, \\ L \sin(\varphi_1) - l_1 \sin(\beta) - l_9 &= 0. \end{aligned} \quad (4)$$

Angle β is obtained from (4) by rearranging and squaring both equations and combining them into one:

$$l_9 \sin(\beta) + l_8 \cos(\beta) = \frac{L^2 - l_1^2 - l_8^2 - l_9^2}{2l_1}. \quad (5)$$

The angle φ_2 is obtained by solving trigonometric Equation (5) for β and inserting it in (3):

$$\varphi_2 = \cos^{-1} \left(\frac{L^2 - l_1^2 - l_8^2 - l_9^2}{2l_1 \sqrt{l_8^2 + l_9^2}} \right) + \tan^{-1} \left(\frac{l_9}{l_8} \right) - \alpha_1. \quad (6)$$

Next, the same procedure is repeated for the second vector loop given with the following equation:

$$l_7e^{j\varphi_3} + l_4e^{j\gamma} - l_{R_6}e^{j\varphi_6} - l_2e^{j\varphi_2} = 0, \quad (7)$$

where angle γ is given as:

$$\gamma = \alpha_2 + \varphi_4. \quad (8)$$

From (7) angle γ is obtained as:

$$k_2 \sin(\gamma) + k_1 \cos(\gamma) = \frac{k_1^2 + k_2^2 + l_4^2 - l_7^2}{2l_4}, \quad (9)$$

where k_1 and k_2 are given as:

$$\begin{aligned} k_1 &= l_8 - l_{10} + l_2 \cos(\varphi_2), \\ k_2 &= l_9 + l_{11} + l_2 \sin(\varphi_2). \end{aligned} \quad (10)$$

By solving trigonometric Equation (9) and inserting it into (8) angle φ_4 is obtained as:

$$\varphi_4 = \cos^{-1} \left(\frac{k_1^2 + k_2^2 + l_4^2 - l_7^2}{2l_4 \sqrt{k_1^2 + k_2^2}} \right) + \tan^{-1} \left(\frac{k_2}{k_1} \right) - \alpha_2. \quad (11)$$

The position of the point P is obtained from the third vector loop as:

$$R_P = R_3 + R_7 + R_8. \quad (12)$$

From (12) coordinates of the point P are obtained as:

$$\begin{aligned} l_{P,x} &= l_8 + l_2 \cos(\varphi_2) + l_6 \cos(\alpha), \\ l_{P,y} &= l_9 + l_2 \sin(\varphi_2) + l_6 \sin(\alpha), \end{aligned} \quad (13)$$

where the angle α is given as:

$$\alpha = \varphi_4 + \alpha_2 + \gamma - 180^\circ. \quad (14)$$

2.3. Virtual Work

The concept of virtual work [28] is used for determining the cylinder force based on given rope force measured in real life scenarios, whose components are F_h and F_v . Two hydraulic cylinders are used for lifting and lowering the skidder rear plate mechanism. Because of that, from [28], the virtual work is given as:

$$\delta W = 2F_{cyl}\delta L + F_h\delta l_{P,x} + F_v\delta l_{P,y} = 0. \tag{15}$$

From (15), the cylinder force is obtained as:

$$2F_{cyl} = -F_h \frac{\partial l_{P,x}}{\partial L} - F_v \frac{\partial l_{P,y}}{\partial L}, \tag{16}$$

where the partial derivatives of position vector p are given as:

$$\begin{aligned} \frac{\partial l_{P,x}}{\partial L} &= -l_2 \sin(\varphi_2) \frac{\partial \varphi_2}{\partial L} - l_6 \sin(\alpha) \frac{\partial \varphi_4}{\partial L}, \\ \frac{\partial l_{P,y}}{\partial L} &= l_2 \cos(\varphi_2) \frac{\partial \varphi_2}{\partial L} + l_6 \cos(\alpha) \frac{\partial \varphi_4}{\partial L}. \end{aligned} \tag{17}$$

In the above expressions, the partial derivatives of angles φ_2 and φ_4 are defined as:

$$\begin{aligned} \frac{\partial \varphi_2}{\partial L} &= -\frac{2L}{2l_1\sqrt{l_8^2 + l_9^2} \sqrt{1 - \frac{(L^2 - l_1^2 - l_8^2 - l_9^2)^2}{(2l_1\sqrt{l_8^2 + l_9^2})^2}}}, \\ \frac{\partial \varphi_4}{\partial L} &= \frac{k}{k_1^2 + k_2^2} - \frac{\frac{k}{l_4} \left(\frac{1}{\sqrt{k_1^2 + k_2^2}} - \frac{k_1^2 + k_2^2 + l_4^2 - l_7^2}{2(k_1^2 + k_2^2)^{\frac{3}{2}}} \right)}{\sqrt{1 - \frac{(k_1^2 + k_2^2 + l_4^2 - l_7^2)^2}{4l_4^2(k_1^2 + k_2^2)}}}, \end{aligned} \tag{18}$$

where k is defined as:

$$k = \frac{\partial \varphi_2}{\partial L} l_2 (k_2 \cos(\varphi_2) - k_1 \sin(\varphi_2)). \tag{19}$$

The horizontal and vertical components of the rope force are given in [29] and are measured for different loads and terrain slopes. The static cylinder forces are calculated using (16) for the given rope force and different cylinder positions. The obtained force profiles are shown in Figure 5. It can be observed that the cylinder forces have almost a linear characteristic, but with different slope coefficients depending on the rope load mass.

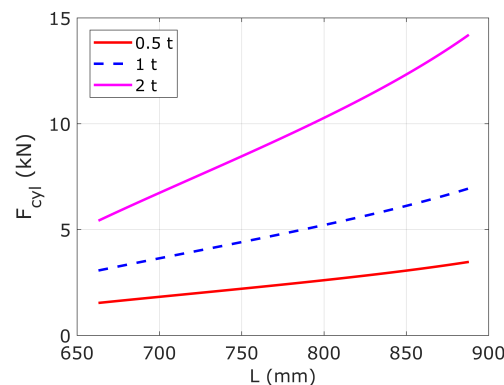


Figure 5. Static profile of cylinder force for different loads.

3. Experimental Setup

The photograph of the experimental setup used in this study and a simplified schematics representation of the setup are shown in Figure 6. The proposed setup is used to test the classical valve-controlled proportional electro-hydraulic system and the DDH system independently but under the same operating conditions. The classical system uses a 1.1 kW AC motor with 1380 rev/min coupled with a 3.7 cm³/rev gear pump for ensuring constant pressure of 60 bar. A proportional valve PRM2 from Argo-Hytos is used for motion control of a double-acting asymmetrical hydraulic cylinder 32/22 × 300 mm with neglectable cylinder losses of approximate value of 1.5%.

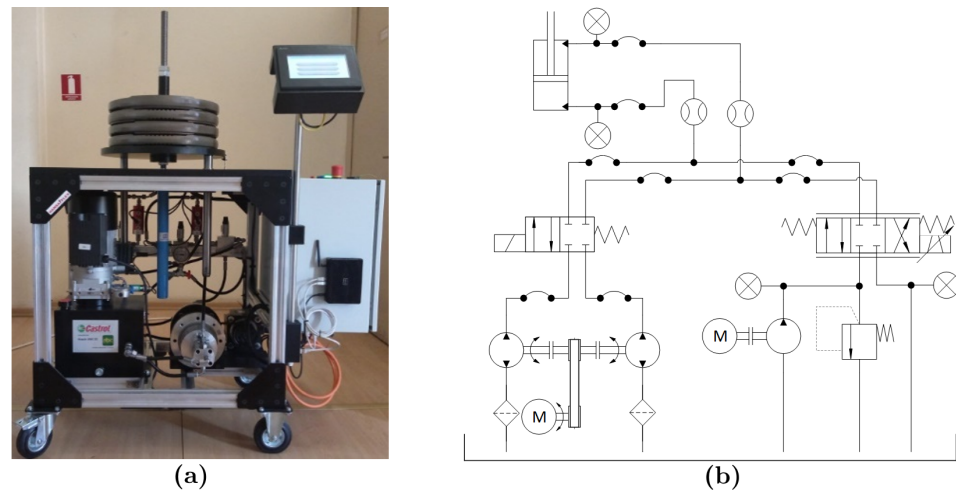


Figure 6. Experimental setup—(a) front view, (b) schematics representation.

The photograph of the DDH drive is shown in Figure 7. It uses two reversible Argo-Hytos gear pumps with a displacement of 4.8 and 2.5 cm³/rev for direct motion control of the hydraulic cylinder. These pumps are mutually connected with the same shaft. A Mitsubishi speed controlled 1.5 kW servo motor with a maximum rotational speed of 2000 rev/min is used for propelling the pumps. For the torque transfer from the servo motor to the pumps, a belt transmission is used. The A-side and B-side pumps create the inlet and outlet flow to the cylinder, where the movement direction of the cylinder depends on the servo motor rotational direction, while the required operating pressure is determined by the payload. The maximum payload of the experimental equipment is estimated to 400 kg and is actually limited by the structural strength of the setup.

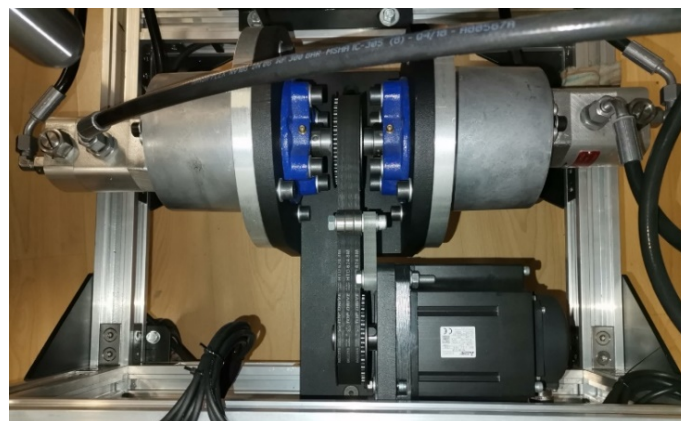


Figure 7. DDH drive.

The experimental setup is designed for easy switching between individual hydraulic systems allowing for an exact comparison of the obtained experimental results. A Wire

Micro-Epsilon WDS sensor is used for measuring the cylinder position, while EVS and HDA sensors from Hydac are used for measuring the inlet flow to and the outlet flow from the cylinder as well as pressures inside the cylinder chambers. The piston velocity is estimated on-line using an algebraic differentiator defined in [30]. Data logging has been performed with a time base (sampling time) of 10 ms, which has been implemented within a Mitsubishi Electric Company's programmable logic controller (PLC) from the MELSEC iQ-F series [31] along with the required hydraulic system control algorithms. Detailed component specifications of the experimental setup are given in Table 1 while detailed system description can be found in [11].

Table 1. Detailed component specifications of the experimental setup.

Component	Model
Cylinder	Hidromehanika $\phi 32/22 \times 300$
Valves (2/2 and 4/2)	ARGO-HYTOS SD2E-A2/L2I12M2-A
Proportional valve	ARGO-HYTOS PRM2-063Z11/8-24EKBK1N2V-A 4/3
A—side pump	ARGO-HYTOS GP1-4.8B-SAVB-SGBGB-N002
B—side pump	ARGO-HYTOS GP1-2.5B-SAVB-SGBGB-N002
Power pack pump	Hydronit gear pump $3.7 \text{ cm}^3/\text{rev}$
AC motor	Končar 5AZCD 90SB-4 B14 F115 1.1 kW
Servo motor	Mitsubishi electric servo motor HG-SN152JK
Motor controller	Mitsubishi electric servo drive MR-JE-200A
Control unit	Mitsubishi electric PLC FX5U-32MT/ESS
Pressure sensors	HYDAC HDA 7446-A-100-000
Flow sensors	HYDAC EVS 3106-A-0020-000
Linear position sensor	MICRO-EPSILON WDS-500-P60-SR-U

4. Experimental Investigation into Energy Efficiency

Both the DDH system and classical hydraulic system have been subjected to loads of 160, 200, 260 and 300 kg, which correspond to load forces of 1.6, 2, 2.6 and 3 kN, respectively. Thus, the experiment with this setup corresponds rather closely to the case of load mass of 0.5 t (see Figure 5). Experimental verification has been done in laboratory conditions with an ambient temperature of 22 °C. The results for both systems are obtained for the stepwise position reference signal where the test cycle consists of three lifting and lowering movements. The duration of the test cycle is one minute.

The input and output energy of the systems are calculated based on the measured data. They are determined based on the power flow direction where the negative work performed by the cylinder is considered as an additional input to the system. Energy efficiency is obtained as a ratio of the output energy to the input energy of the system, and these values are illustrated in Figure 8. While the cylinder is pulled out, the system input consists of the power from an electric motor or a servo-motor only, depending on the hydraulic system being used. In the case when the cylinder is pulled in, additional input power emerges from the potential energy of the load. Consequently, the input system energy is defined as the sum of integrals of all input powers and the output system energy as an integral of output power from [22] as:

$$E_{in} = \int P_{in,i} dt + \int \left| P_{cyl} \right| \Big|_{P_{cyl} < 0} dt, \quad (20)$$

$$E_{out} = \int P_{cyl} \Big|_{P_{cyl} \geq 0} dt, \quad (21)$$

where $P_{in,i}$ is the input electrical power and index i represents either the DDH or the classical system and P_{cyl} is power from the hydraulic cylinder. In every time stamp the PLC gets information on the servo-motor input power for the DDH system. For the classical

system, the current input power is calculated for the single-phase AC electric motor from the measured and catalogue data:

$$P_{in,AC} = U_{eff} I \cos(\varphi), \quad (22)$$

where U_{eff} is the effective voltage, $\cos(\varphi)$ is the power factor taken from the datasheet having the rated value of 0.92 for the particular electrical motor, and I is measured effective current through the electric motor. Hydraulic cylinder power P_{cyl} is calculated from estimated piston velocity v , measured pressures inside two cylinder chambers p_A and p_B , and its areas A_A and A_B from [12] as:

$$P_{cyl} = (p_A A_A - p_B A_B) v. \quad (23)$$

The results in Figure 8 clearly indicate that the DDH system can achieve much higher energy efficiency in comparison to the classical hydraulic system.

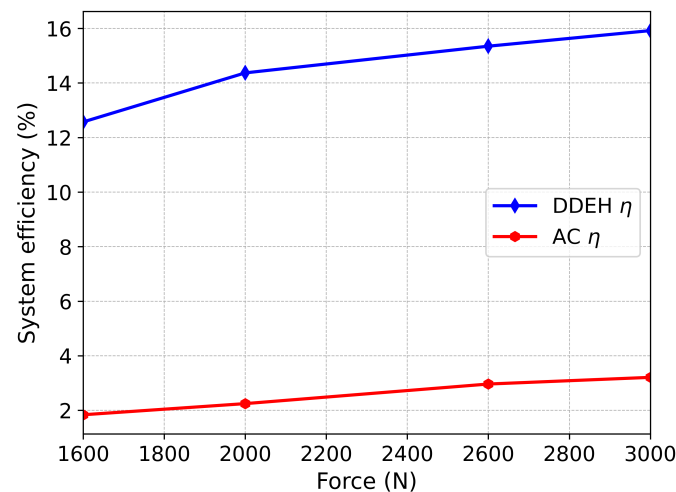


Figure 8. System efficiency for static loads.

The output energy of both systems is equal due to the same load conditions as shown in Table 2. The main difference occurs between input energies. The classical system gives the constant input pressure set by the safety valve while the pressure inside the DDH system is determined by the cylinder load. Because of that, the DDH system uses about five times less energy for lifting and lowering movements of the same loads.

Table 2. System energy consumption for static loads.

	F (kN)	1.6	2	2.6	3
Classical system	E_{in} (kJ)	77.8	78.7	80	80
	E_{out} (kJ)	1.4	1.7	2.3	2.5
DDH system	E_{in} (kJ)	11.4	12.3	15.1	16.2
	E_{out} (kJ)	1.4	1.7	2.3	2.5

5. Discussion

In the optimal operating point, as defined in [4], the specific fuel consumption q of the skidder diesel engine powerplant is between 200 and 214 g/kWh. According to the EN 590 standard density ρ of diesel fuel is in the range from 0.82 to 0.845 kg/L. The average values of

the skidder specific fuel consumption and fuel density are used to calculate the equivalent fuel consumption FL needed to obtain the previously calculated input energy E_{in} :

$$FL = \frac{E_{in}}{3600} \times q \times \frac{1}{\rho}. \quad (24)$$

with the current fuel net price CP of 1.40 EUR/L for diesel fuel, the number of lowering and lifting cycles per day n and workdays per year wpy presented in Table 3, fuel price FP is calculated as follows:

$$FP = FL \times n \times wpy \times CP. \quad (25)$$

The cost of a proportional hydraulic valve for the classical system is around 1000 EUR, which is equal to the cost of a the servomotor within the DDH system. The cost of two reversible hydraulic pumps used in this experimental setup is around 350 EUR. With a yearly fuel savings of 85.05 EUR, the proposed system reaches the break-even point (return-of-investment point) in 4.12 years if the price difference of 350 EUR between the classical and the DDH system is not exceeded.

Table 3. System fuel consumption.

	E_{in} (kJ)	Fuel Consumption (L)	Lowering/Lifting Cycles per Day	Workdays per Year	Fuel Price (EUR)
Classical system	80	0.0056	54	250	105.84
DDH system	16.2	0.0011	54	250	20.79

Note that by implementing the proposed DDH system within the skidder, some extra weight is added, which only slightly increases fuel consumption. Note also that the location of the proposed system should be carefully chosen on the skidder and protected from external factors because tree branches can easily damage electrical wiring and hydraulic lines.

6. Conclusions

The paper has analysed the potential uses of the direct driven hydraulic system for the skidder rear plate mechanism positioning task. The analysis of the rear plate linkage mechanism position vs. force arm dependence was performed using vector loops approach, whereas cylinder forces were calculated using the principle of virtual work. Based on the aforementioned relationships, energy efficiency was obtained as a ratio of the input energy to the output energy of the system. The performance of the classical and direct driven hydraulic system has been analysed for four different loads using the existing hydraulic system experimental setup.

The results indicate that the use of the proposed direct driven hydraulic system would significantly increase the energy and fuel efficiency of the skidder for the considered operating regime, i.e., it can be expected that fuel expenditure may be reduced up to five times compared to the case of utilisation of the on-board (conventional) hydraulics currently in use. In addition, even higher energy efficiency could be achieved if the potential energy of the load is used for lowering manoeuvres, because in that case the potential energy of the load could be converted back into electrical energy and stored in batteries. Based on the obtained results and assumed skidder operating regimes, the return of the investment period for the case of direct drive hydraulic system retrofitting should be about four years.

The paper also shows that with the proposed DDH system, the skidder front plate, and the steering mechanism could be also replaced. A direct consequence of this replacement is an additional improvement in energy efficiency of the skidder, which, in turn, enables further downsizing of the internal combustion engine without sacrificing the hydraulic drive performance. Finally, the analysis has also shown that the hydraulic circuit can be greatly simplified by removing proportional valves and high-pressure filters, which are needed within the conventional hydraulic system. By removing these components, the

reliability of the overall hydraulic system would be notably increased, thus resulting in less maintenance time and lower maintenance costs.

Further work is going to be directed towards the implementation of the DDH system within the hybrid drive-based skidder, followed by a detailed field study under realistic log hauling operating conditions during harvesting, along with the derivation of dynamic models for DDH and proportional hydraulics for skidder application for future comparative analyses.

Author Contributions: Conceptualization, J.B. and J.K.; methodology, J.B. and J.K.; software, J.B.; validation, J.B., J.K. and M.C.; formal analysis, J.K. and J.B.; investigation, J.B. and J.K.; resources, J.B.; writing—original draft preparation, J.B. and J.K.; writing—review and editing, D.P., Ž.Š. and M.C.; visualization, M.C.; supervision, Ž.Š.; project administration, Ž.Š.; funding acquisition, Ž.Š. All authors have read and agreed to the published version of the manuscript.

Funding: This research was funded by the European Regional Development Fund under the grant KK.01.1.1.04.0010 (HiSkid).

Institutional Review Board Statement: Not applicable.

Informed Consent Statement: Not applicable.

Data Availability Statement: Research data can be made available for non-profit use in research and education upon a formal request made to the corresponding author.

Acknowledgments: Authors gratefully acknowledge assistance of M. Čavka from Hidromehanika d.o.o, H. Zidar from ABC maziva d.o.o. and O. Tomić from HANSA-FLEX Croatia d.o.o. who greatly contributed to the development of this laboratory model and provided their assistance in the hardware setup.

Conflicts of Interest: The authors declare no conflict of interest.

Nomenclature

Symbol	Description
A_A, A_B	piston areas
CP	current fuel price
E_{in}	input energy
E_{out}	output energy
F_{cyl}	cylinder force
F_h	horizontal force
F_v	vertical force
FL	equivalent fuel consumption
FP	fuel price
L	cylinder length
l_i	link length
$l_{P,x}, l_{P,y}$	x and y position of point P
n	lifting cycles per day
p_A, p_B	pressure inside cylinder chambers
$P_{in,i}$	input power of the system
P_{cyl}	cylinder power
q	specific fuel consumption
R_i	position vectors
v	piston velocity
W	virtual work
wpy	workdays per year
$\alpha_i, \beta_i, \gamma_i$	angles of triangle links
φ_i	link angle
ρ	fuel density

References

1. Fonseca, A.; Aghazadeh, F.; de Hoop, C.; Ikuma, L.; Al-Qaisi, S. Effect of noise emitted by forestry equipment on workers' hearing capacity. *Int. J. Ind. Ergon.* **2015**, *46*, 105–112. [[CrossRef](#)]
2. Potočnik, I.; Poje, A. Forestry ergonomics and occupational safety in high ranking scientific journals from 2005–2016. *Croat. J. For. Eng. J. Theory Appl. For. Eng.* **2017**, *38*, 291–310.
3. Rong-Feng, S.; Xiaozhen, Z.; Chengjun, Z. Study on Drive System of Hybrid Tree Harvester. *Sci. World J.* **2017**, *2017*, 8636204. [[CrossRef](#)] [[PubMed](#)]
4. Karlušić, J.; Cipek, M.; Pavković, D.; Benić, J.; Šitum, Ž.; Pandur, Z.; Šušnjar, M. Simulation Models of Skidder Conventional and Hybrid Drive. *Forests* **2020**, *11*, 921. [[CrossRef](#)]
5. Karlušić, J.; Cipek, M.; Pavković, D.; Šitum, Ž.; Benić, J.; Šušnjar, M. Benefit Assessment of Skidder Powertrain Hybridization Utilizing a Novel Cascade Optimization Algorithm. *Sustainability* **2020**, *12*, 10396. [[CrossRef](#)]
6. Knežević, I. Preoblikovanje Razvodnika Dnage šumskog Traktora za Pogon svih kotača i Vitla (Reshaping Power Distributor of Skidder to Drive all the Wheels and Winches). Master's Thesis, University of Zagreb, Zagreb, Croatia, 2010.
7. Gillich, N.; Širbu, N.; Vlase, S.; Marin, M. Study of Metallic Housing of the Adder Gearbox to Reduce the Noise and to Improve the Design Solution. *Metals* **2021**, *11*, 912. [[CrossRef](#)]
8. Solazzi, L. Design and experimental tests on hydraulic actuator made of composite material. *Compos. Struct.* **2020**, *232*, 111544. [[CrossRef](#)]
9. Torregrossa, D.; Capitanescu, F. Optimization models to save energy and enlarge the operational life of water pumping systems. *J. Clean. Prod.* **2019**, *213*, 89–98. [[CrossRef](#)]
10. Bagirov, A.; Ahmed, S.; Barton, A.; Mala-Jetmarova, H.; Al Nuaimat, A.; Sultanova, N.; GWMWater, H. Comparison of metaheuristic algorithms for pump operation optimization. In Proceedings of the Water Distribution Systems Analysis Conference, Adelaide, Australia, 24–27 September 2012; pp. 886–896.
11. Benić, J.; Šitum, Ž. Position Controller for Direct Driven Electro-Hydraulic System. In Proceedings of the International Conference Fluid Power 2019: Conference Proceedings, Tampere, Finland, 22–24 May 2019. [[CrossRef](#)]
12. Agostini, T.; Negri, V.D.; Minav, T.; Pietola, M. Effect of Energy Recovery on Efficiency in Electro-Hydrostatic Closed System for Differential Actuator. *Actuators* **2020**, *9*, 12. [[CrossRef](#)]
13. Turunen, A.; Minav, T.; Hanninen, H.; Pietola, M. Experimental Investigation of Direct Drive Hydraulic Units Implemented in a Mining Loader. In Proceedings of the 2018 Global Fluid Power Society PhD Symposium (GFPS), Samara, Russia, 18–20 July 2018; pp. 1–6. [[CrossRef](#)]
14. Cerman, O.; Hušek, P. Adaptive fuzzy sliding mode control for electro-hydraulic servo mechanism. *Expert Syst. Appl.* **2012**, *39*, 10269–10277. [[CrossRef](#)]
15. Cukla, A.R.; Izquierdo, R.; Borges, F.A.; Perondi, E.A.; Lorini, F.J. Optimum Cascade Control Tuning of a Hydraulic Actuator Based on Firefly Metaheuristic Algorithm. *IEEE Lat. Am. Trans.* **2018**, *16*, 384–390. [[CrossRef](#)]
16. dos Santos Coelho, L.; Cunha, M.A.B. Adaptive cascade control of a hydraulic actuator with an adaptive dead-zone compensation and optimization based on evolutionary algorithms. *Expert Syst. Appl.* **2011**, *38*, 12262–12269. [[CrossRef](#)]
17. Wang, R.; Tan, C.; Xu, J.; Wang, Z.; Jin, J.; Man, Y. Pressure Control for a Hydraulic Cylinder Based on a Self-Tuning PID Controller Optimized by a Hybrid Optimization Algorithm. *Algorithms* **2017**, *10*, 19. [[CrossRef](#)]
18. Niraula, A.; Zhang, S.; Minav, T.; Pietola, M. Effect of Zonal Hydraulics on Energy Consumption and Boom Structure of a Micro-Excavator. *Energies* **2018**, *11*, 2088. [[CrossRef](#)]
19. Zhang, S.; Minav, T.; Pietola, M. Decentralized Hydraulics for Micro Excavator. In Proceedings of the 15th Scandinavian International Conference on Fluid Power (SICFP'17), Linköping, Sweden, 7–9 June 2017; pp. 187–195.
20. Minav, T.; Bonato, C.; Sainio, P.; Pietola, M. Direct Driven Hydraulic Drive. In Proceedings of the 9th International Fluid Power Conference (9. IFK), Aachen, Germany, 24–26 March 2014; pp. 508–517.
21. Minav, T.; Heikkinen, J.; Schimmel, T.; Pietola, M. Direct Driven Hydraulic Drive: Effect of Oil on Efficiency in Sub-Zero Conditions. *Energies* **2019**, *12*, 219. [[CrossRef](#)]
22. Benić, J.; Šitum, Ž.; Cipek, M.; Pavković, D.; Kasać, J. Comparison of Sliding Mode Controller for Classical and Direct Driven Electrohydraulic System. In Proceedings of the Scandinavian International Conference on Fluid Power, Linköping, Sweden, 31 May–2 June 2021; pp. 26–35.
23. Benić, J.; Karlušić, J.; Šitum, Ž.; Cipek, M.; Pavković, D. Potential Use of Novel Efficient Direct Driven Electro-Hydraulic System for Skidders. In Proceedings of the 16th Conference on Sustainable Development of Energy, Water and Environment Systems (SDEWES), Dubrovnik, Croatia, 10–15 October 2021.
24. Prasanna, G.K. Geometric performance parameters of three-point hitch linkage system of a 2WD Indian tractor. *Res. Agric. Eng.* **2016**, *61*, 47–53. [[CrossRef](#)]
25. Pan, Y.C.; Cai, G.W.; Zhang, Z.; Chen, Y.; Li, Y.Z. Kinematics and Kinetostatic Analysis of a New Type of Mechanical Excavator with Controllable Mechanism. *Appl. Mech. Mater.* **2011**, *141*, 334–338. [[CrossRef](#)]
26. Hittner d.o.o. Available online: <http://hittner.hr/> (accessed on 23 November 2021).
27. Development of Hybrid Skidder: HiSkid. Available online: <https://www.hiskid.hr/> (accessed on 23 November 2021).
28. Norton, R. *Design of Machinery: An Introduction to the Synthesis and Analysis of Mechanisms and Machines*; McGraw-Hill Higher Education: Boston, MA, USA, 2004.

29. Đuka, A.; Pentek, T.; Horvat, D.; Poršinsky, T. Modelling of Downhill timber skidding: Bigger load–bigger slope. *Croat. J. For. Eng. J. Theory Appl. For. Eng.* **2016**, *37*, 139–150.
30. Kasac, J.; Majetic, D.; Brezak, D. An algebraic approach to on-line signal denoising and derivatives estimation. *J. Frankl. Inst.* **2018**, *355*, 7799–7825. [[CrossRef](#)]
31. MELSEC iQ-F Series. Available online: <https://www.mitsubishielectric.com/fa/products/cnt/plcf/items/index.html> (accessed on 23 November 2021).